Localization-Free Power Cartography

Yves Teganya, Luis Miguel Lopez-Ramos, Daniel Romero,
and Baltasar Beferull-Lozano

Abstract **—Spectrum cartography constructs maps of metrics such as channel gain or received signal power across a geographic area of interest using measurements of spatially distributed sensors. Applications of these maps include network planning, interference coordination, power control, localization, and cognitive radio to name a few. Existing spectrum cartography methods necessitate knowledge of sensor locations, but such locations cannot be accurately determined from pilot positioning signals (such as those in LTE or GPS) in indoor or dense urban scenarios due to multipath. To circumvent this limitation, this paper proposes localization-free cartography, where spectral maps are directly constructed from features of these positioning signals rather than from location estimates. The proposed algorithm capitalizes on the framework of kernel-based learning and offers improved prediction performance relative to existing alternatives, as demonstrated by a simulation study in a street canyon.**

Keywords— Spectrum cartography, localization-free cartography, kernel-based learning, spectrum map.

A.1 Introduction

Spectrum cartography constructs maps of a certain channel metric, such as received signal power, interference power, or channel gain over the geographical area of interest [1–3]. Spectral maps are of utmost interest in wireless networks, especially for tasks such as network planning, interference coordination, power control, and dynamic spectrum access [4–6]. Further applications include source localization [2].

Existing approaches typically apply some spatial interpolation or regression technique to measurements collected by spatially distributed sensors. Examples of these approaches for mapping power over space include kriging [1, 7, 8], compressive sensing [3], matrix completion [9], dictionary learning [10, 11], Bayesian models [12], and adaptive radial basis functions [13]. Schemes to map power spectral density (PSD) have also been devised by exploiting the sparsity of power distribution over space and frequency [2] and by leveraging the frameworks of thin-plate spline regression [4, 14] and kernel-based learning [4]. Further schemes have been proposed to map alternative metrics such as channel gain [15–17].

Since all the aforementioned schemes rely on the knowledge of the sensor locations, they will be collectively referred to as *localization-based cartography*. In practice, location is seldom known and therefore it must be estimated from features such as the RSSI, the time (difference) of arrival, or the direction of arrival of positioning pilot signals transmitted by satellites (e.g. in GPS) or terrestrial base stations (e.g. in LTE or

WiFi [18]). Unfortunately, accurate location estimates are often not available in practice due to propagation phenomena affecting those pilot signals such as multipath, which limits the applicability of existing cartography techniques, especially in indoor and dense urban scenarios.

The main contribution of this paper is to circumvent this limitation by proposing localization-free cartography. The idea is that the localization step introduces significant errors in the spectrum map estimation when the aforementioned features are not reliable. Bypassing this step, the proposed approach obtains spectrum maps indexed directly by (or as a function of) the features of the received pilots. As a byproduct of skipping the localization step, the resulting cartography algorithm is also computationally less expensive than its localization-based counterparts. For simplicity, this work focuses on constructing power maps, but the proposed algorithm carries over to other metrics. Such an algorithm is developed within the framework of kernel-based learning not only because of the high simplicity, flexibility, and performance of kernel-based estimators, but also because it has well-documented merits in spectrum cartography [4, 14].

The rest of this paper is organized as follows: Sec. A.2 describes the problem and reviews location-based cartography. Sec. A.3 presents the main contribution of the paper, which is localization-free cartography. Simulations and conclusions are respectively provided in Sec. A.4 and Sec. A.5.

A.2 Preliminaries

The goal is to determine the power $p(\boldsymbol{x})$ of a certain channel, termed *channel-to-map* (C2M), at every location $\boldsymbol{x} \in \mathcal{X}$ of the geographical region $\mathcal{X} \subset \mathbb{R}^2$ of interest. To this end, N sensors are deployed across $\mathcal{X}$ at locations $\{\boldsymbol{x}_n\}_{n=1}^N$ not necessarily known. The n-th sensor acquires a measurement $\tilde{p}_n$ of the power $p(\boldsymbol{x}_n)$ at its location $\boldsymbol{x}_n$.

In localization-based cartography, a fusion center is ideally given pairs $\{(\boldsymbol{x}_n, \tilde{p}_n)\}_{n=1}^N$, which include the exact sensor locations $\{\boldsymbol{x}_n\}_{n=1}^N$, and obtains a function estimate $\hat{p}(\boldsymbol{x}_q)$ that provides the power of the C2M at any query location $\boldsymbol{x}_q \in \mathcal{X}$. With this function, a node at $\boldsymbol{x}_q$ can determine the power of the C2M if it knows $\boldsymbol{x}_q$. In practice, however, location is typically unknown and hence the n-th sensor must estimate $\boldsymbol{x}_n$ by relying on pilot signals $\{y_{m,n}[k]\}_{m=1}^M$, where $y_{m,n}[k]$ denotes the k-th sample of the m-th pilot signal received by the n-th sensor. For convenience, form the $M \times K$ matrix $\boldsymbol{Y}_n$ whose (m,k)-th entry is $y_{m,n}[k]$. From $\boldsymbol{Y}_n$, the n-th sensor computes an estimate $\hat{\boldsymbol{x}}_n(\boldsymbol{Y}_n)$ of $\boldsymbol{x}_n$ by means of some localization algorithm; see Sec. A.4 for a specific example. The fusion center then uses $\{(\hat{\boldsymbol{x}}_n, \tilde{p}_n)\}_{n=1}^N$ to obtain an estimate $\hat{p}(\boldsymbol{x})$ of the function $p(\boldsymbol{x})$. Therefore, if the location estimates $\{\hat{\boldsymbol{x}}_n\}_{n=1}^N$ are noisy, so will be $\hat{p}(\boldsymbol{x})$. If a node at a query location $\boldsymbol{x}_q$ wishes to know the power of the C2M, it will use the pilot signals $\boldsymbol{Y}_q$ to obtain an estimate $\hat{\boldsymbol{x}}_q := \hat{\boldsymbol{x}}(\boldsymbol{Y}_q)$ of its location and will evaluate the map estimate as $\hat{p}(\hat{\boldsymbol{x}}_q)$. Here, $\boldsymbol{Y}_q$ is a matrix whose (m,k)-th entry is given by the k-th sample of the m-th pilot signal $y_{m,q}[k]$ at the query location $\boldsymbol{x}_q$. Thus, such an evaluation has two sources of error: first, the location estimation error in $\hat{\boldsymbol{x}}_q$ and, second, the map estimation error in $\hat{p}(\boldsymbol{x}_q)$.

From a more general perspective, the function that is actually learned in this approach

can be expressed as $p(\boldsymbol{Y}) := p(\hat{\boldsymbol{x}}(\boldsymbol{Y}))$, where $\hat{\boldsymbol{x}}(\boldsymbol{Y})$ denotes the output of the chosen localization algorithm when the pilot signals are given by $\boldsymbol{Y}$. From this perspective, the problem that is being solved is: given $\{(\boldsymbol{Y}_n, \tilde{p}_n)\}_{n=1}^N$, find an estimate $\hat{p}(\boldsymbol{Y})$ of $p(\boldsymbol{Y})$. Indeed, localization-based cartography seeks an estimate for the latter function within a certain family of functions that can be expressed as $p(\boldsymbol{Y}) = g(\hat{\boldsymbol{x}}(\boldsymbol{Y}))$ for some function $g : \mathcal{X} \to \mathbb{R}$. The next section investigates estimates with alternative forms, which will be preferable whenever $\hat{\boldsymbol{x}}(\boldsymbol{Y})$ is not an accurate estimator of $\boldsymbol{x}$.

Remark 1 *One may argue that a node can determine the power of the C2M at its location more efficiently by measuring it rather than by locating itself and evaluating a map. While this may be the case for a single C2M, determining the power of many C2Ms, or other channel parameters such as the impulse response, may incur a higher cost. In these cases, the benefits of spectrum cartography would be more significant.*

A.3 Localization-free Cartography

This section proposes localization-free cartography, which bypasses the localization step involved in all existing cartography approaches. To this end, the localization-free cartography problem is formulated as a function estimation task in Sec. A.3.1 and solved via kernel-based learning in Sec. A.3.2.

A.3.1 Map Estimate as a Function Composition

From an abstract perspective, spectrum cartography amounts to learning a function $p : \mathbb{C}^{M\times K} \to \mathbb{R}$ that provides the power $p(\boldsymbol{Y})$ of the C2M at a location in $\mathcal{X}$ where the pilot signals $\boldsymbol{Y}$ are received. The *direct approach* to spectrum cartography would be to learn such a function directly from data $\{(\boldsymbol{Y}_n, \tilde{p}_n)\}_{n=1}^N$. Since learning a multivariate function up to a reasonable accuracy generally requires the number of data points to be several times larger than the number of input variables, the direct approach would need N to be significantly larger than MK, which is prohibitively large since MK is typically in the order of hundreds or thousands. For this reason, existing (localization-based) cartography schemes do not follow such a direct approach. Instead, they avoid its complexity by confining the search for estimates of $p(\boldsymbol{Y})$ to those functions that can be expressed as the composition of a fixed function $\hat{\boldsymbol{x}} : \mathbb{C}^{M\times K} \to \mathcal{X} \subset \mathbb{R}^2$, where $\hat{\boldsymbol{x}}(\boldsymbol{Y})$ corresponds to the output of a localization algorithm when the pilot signals are $\boldsymbol{Y}$, and a map function $g : \mathcal{X} \subset \mathbb{R}^2 \to \mathbb{R}$ that needs to be determined; (cf. Sec. A.2). Clearly, finding g requires a significantly smaller N than learning the general function $p : \mathbb{C}^{M\times K} \to \mathbb{R}$ since g has only two scalar inputs. When $\hat{\boldsymbol{x}}(\boldsymbol{Y})$ is a reasonable estimate of the location $\boldsymbol{x}$ at which $\boldsymbol{Y}$ has been observed, such a localization-based approach works well. However, due to propagation effects impacting the pilot signals in $\boldsymbol{Y}$, $\hat{\boldsymbol{x}}(\boldsymbol{Y})$ may be very different from $\boldsymbol{x}$ and it is easy to see that this drastically hinders the estimation of g. From this observation, it can be concluded that the two scalar outputs of $\hat{\boldsymbol{x}}(\boldsymbol{Y})$ fail to capture the relevant information in $\boldsymbol{Y}$: more outputs are needed. In summary, neither the above direct approach, which estimates a function with MK inputs, nor the localization-based

approach, which estimates a function of 2 inputs, are appropriate in presence of multipath effects, as is the case in indoors or urban scenarios.

To tackle this difficulty, the proposed approach is to estimate a function whose number of inputs is larger than 2 and smaller than MK. To answer the question on which inputs should be used, it is worth delving further into why the above localization-based approach fails. Localization algorithms typically proceed in two steps: first, they extract some *features* from $\boldsymbol{Y}$, and then they feed these features to an algorithm L that exploits a spatial model to determine the location. Those features comprise e.g. estimates of distance, time (difference) of arrival, or angle of arrival. If $\boldsymbol{\phi}(\boldsymbol{Y}) \in \mathcal{D} \subset \mathbb{R}^M$ denotes the vector stacking these M features and $\boldsymbol{l}(\boldsymbol{\phi})$ denotes the output of algorithm L, it follows that $\hat{\boldsymbol{x}}(\boldsymbol{Y}) = \boldsymbol{l}(\boldsymbol{\phi}(\boldsymbol{Y}))$. The root of the problem is therefore that the model assumed by L is inaccurate: it typically assumes free space propagation, which would imply a certain consistency between the features in $\boldsymbol{\phi}(\boldsymbol{Y})$ that does not hold in presence of multipath. Combining these observations, a sensible approach is to (i) preserve the dimensionality reduction capability of $\boldsymbol{\phi}$ (from MK to M); and (ii) avoid the error introduced by $\boldsymbol{l}(\boldsymbol{\phi})$. Thus, one can seek *localization-free* function estimates of the form $\hat{p}^{\mathrm{LF}}(\boldsymbol{Y}) = f(\boldsymbol{\phi}(\boldsymbol{Y}))$ for some $f : \mathcal{D} \subset \mathbb{R}^M \to \mathbb{R}$. In this localization-free setup, $\boldsymbol{\phi}(\boldsymbol{Y})$ comprises M features of the pilot signals, but they need not be those used by the localization algorithms (e.g. time (difference) or angle of arrival). In short, whereas localization-based cartography learns a function of the spatial location estimated from features of the pilot signals, the proposed localization-free approach directly learns a function of such features.

A.3.2 Kernel-based Power Map Learning

This section provides a kernel-based learning algorithm to learn the function f introduced in Sec. A.3.1. Given pairs $\{(\boldsymbol{\phi}_n, \tilde{p}_n)\}_{n=1}^N$, where $\boldsymbol{\phi}_n := \boldsymbol{\phi}(\boldsymbol{Y}_n)$, the regression problem is informally to find f such that $f(\boldsymbol{\phi}(\boldsymbol{Y})) \approx p(\boldsymbol{Y})$ for all $\boldsymbol{Y}$. To address this problem, one must specify in which family of functions such an f must be found. In kernel-based learning, one seeks f in a set known as a *reproducing-kernel Hilbert space* (RKHS) and given by

$$\mathcal{F} := \left\{ f : f(\boldsymbol{\phi}) = \sum_{i=1}^{\infty} \alpha_i \kappa(\boldsymbol{\phi}, \bar{\boldsymbol{\phi}}_i),\ \bar{\boldsymbol{\phi}}_i \in \mathcal{D},\ \alpha_i \in \mathbb{R} \right\},$$

where $\kappa : \mathcal{D} \times \mathcal{D} \to \mathbb{R}$ is a symmetric and positive definite function known as *reproducing kernel* [19]. A common choice is the so-called Gaussian *radial basis function* $\kappa(\boldsymbol{\phi}, \boldsymbol{\phi}') := \exp\left[-\|\boldsymbol{\phi} - \boldsymbol{\phi}'\|^2/(2\sigma^2)\right]$, where σ is a parameter selected by the user. Like any Hilbert space, $\mathcal{F}$ has an associated inner product and norm. For an RKHS function $f(\boldsymbol{\phi}) = \sum_{i=1}^{\infty} \alpha_i \kappa(\boldsymbol{\phi}, \bar{\boldsymbol{\phi}}_i)$, the latter is given by

$$\|f\|_{\mathcal{F}}^2 := \sum_{i=1}^{\infty} \sum_{j=1}^{\infty} \alpha_i \alpha_j \kappa(\bar{\boldsymbol{\phi}}_i, \bar{\boldsymbol{\phi}}_j). \tag{A.1}$$

Kernel-based learning typically solves a problem of the form

$$\hat{f} = \arg\min_{f \in \mathcal{F}} \frac{1}{N} \sum_{n=1}^{N} \mathcal{L}\left(\tilde{p}_n, \boldsymbol{\phi}_n, f(\boldsymbol{\phi}_n)\right) + \Omega(\|f\|_{\mathcal{F}}), \tag{A.2}$$

where $\mathcal{L}$ is a loss function quantifying the deviation between the observations $\{\tilde{p}_n\}_{n=1}^N$ and the predictions $\{f(\boldsymbol{\phi}_n)\}_{n=1}^N$ returned by a candidate f; and Ω is an increasing function. The first term in (A.2) promotes function estimates that fit well the data whereas the second term promotes "smooth" estimates; where the notion of smoothness is determined by the RKHS norm $\|\cdot\|_{\mathcal{F}}$. Typical choices are $\mathcal{L}\left(\tilde{p}_n, \boldsymbol{\phi}_n, f(\boldsymbol{\phi}_n)\right) = (\tilde{p}_n - f(\boldsymbol{\phi}_n))^2$ and $\Omega(\|f\|_{\mathcal{F}}) = \lambda \|f\|_{\mathcal{F}}^2$, where $\lambda > 0$ is termed regularization parameter and balances smoothness and goodness of fit. For this choice, $\hat{f}$ is termed *kernel ridge regression* estimate [20], and is the one pursued here for simplicity. The goal is therefore to solve (A.2). However, since $\mathcal{F}$ is infinite dimensional in general, (A.2) cannot be directly solved. Fortunately, one can invoke the *representer theorem* [19], which states that the solution to (A.2) is of the form

$$\hat{f}(\boldsymbol{\phi}) = \sum_{n=1}^{N} \alpha_n \kappa(\boldsymbol{\phi}, \boldsymbol{\phi}_n). \tag{A.3}$$

for some $\{\alpha_n\}_{n=1}^N$. Although the representer theorem does not provide the coefficients $\{\alpha_n\}_{n=1}^N$, they can be obtained by substituting (A.3) into (A.2) and solving the resulting problem with respect to these coefficients. Applying this procedure for kernel ridge regression results in the problem

$$\hat{\boldsymbol{\alpha}} = \arg\min_{\boldsymbol{\alpha}} \frac{1}{N} \|\tilde{\boldsymbol{p}} - \boldsymbol{K}\boldsymbol{\alpha}\|^2 + \lambda \boldsymbol{\alpha}^\top \boldsymbol{K} \boldsymbol{\alpha}, \tag{A.4}$$

where $\boldsymbol{\alpha} := [\alpha_1, ..., \alpha_N]^\top$, $\tilde{\boldsymbol{p}} := [\tilde{p}_1, ..., \tilde{p}_N]^\top$, and $\boldsymbol{K}$ is an $N \times N$ matrix whose (n, n')-th entry is $\kappa(\boldsymbol{\phi}_n, \boldsymbol{\phi}_{n'})$. Problem (A.4) can be solved in closed form as

$$\hat{\boldsymbol{\alpha}} = (\mathbf{K} + \lambda N \mathbf{I}_N)^{-1} \tilde{\boldsymbol{p}}. \tag{A.5}$$

The estimate $\hat{f}$ solving (A.2) for kernel ridge regression can be recovered by substituting (A.5) into (A.3). To obtain the predicted power of the C2M at a query location $\boldsymbol{x}_q$ where the pilot signals are given by $\boldsymbol{Y}_q$, one just evaluates $\hat{p}^{\mathrm{LF}}(\boldsymbol{Y}_q) = \hat{f}(\boldsymbol{\phi}(\boldsymbol{Y}_q))$.

A.4 Numerical tests

This section evaluates the performance of localization-free cartography in a scenario with multipath. The latter is a *urban canyon* or *street canyon*, which comprises two parallel vertical planes modeling the walls (or buildings) at each side of the street and a horizontal plane modeling the ground. Propagation is characterized by the so called *six-ray model* [21], which accounts for the direct path, the ground reflection, 2 first-order wall reflections, and 2 wall-to-wall second-order reflections. The sensors are spread uniformly at random over the street, which is 250 m long and 30 m wide.

For simplicity, the pilot signals are impulses centered at time 0 filtered to the pilot channel with bandwidth 5 MHz and carrier frequency 800 MHz, which implies that $\boldsymbol{Y}_n$ comprises the impulse responses of the bandlimited channels between the M transmitters of pilot signals and the n-th sensor. For simplicity and robustness to timing errors, the

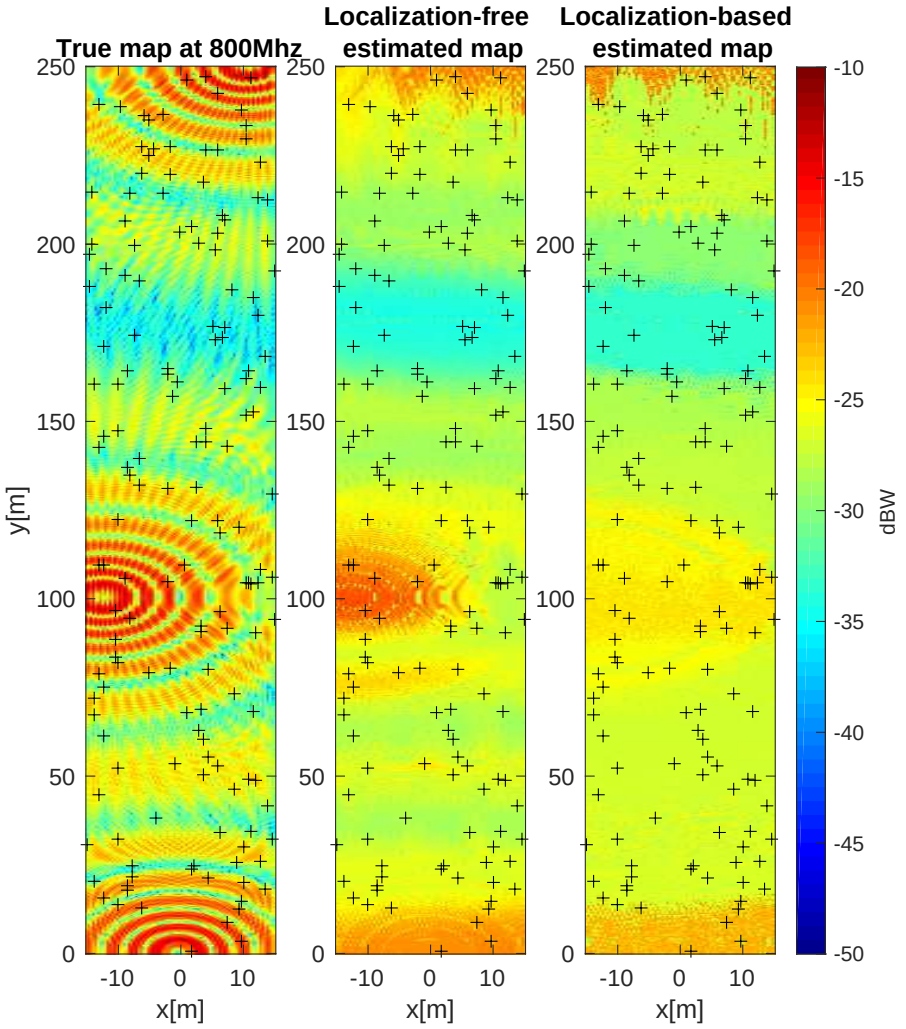

Figure A.1: (a) True map, (b) localization-free, and (c) localization-based estimated maps ($\lambda = 3 \times 10^{-3}$, $N = 160$).

features used by the proposed localization-free algorithm equal the center of mass of the corresponding impulse responses, that is,

$$[\boldsymbol{\phi}_n]_m := \frac{\sum_{k=1}^{K} t_k |y_{m,n}[k]|^2}{\sum_{k=1}^{K} |y_{m,n}[k]|^2},$$

where t_k is the time of the k-th sample.

The proposed algorithm, which uses Gaussian radial basis functions with $\sigma = 30$ m, is compared with its localization-based counterpart, which is a special case of the estimators in [2, 4, 22] for estimating power maps. We use Gaussian RBFs because they are universal kernels [23], i.e., able to approximate arbitrary functions. For localization, the *square-range-based least squares* (SR-LS) algorithm [24] is applied to the time-of-arrival measurements obtained from the pilots $\{\boldsymbol{Y}_n\}_{n=1}^{N}$. Function g (cf. Sec. A.2) is obtained by applying a similar procedure as in the proposed localization-free algorithm: Given $\{(\hat{\boldsymbol{x}}_n, \tilde{p}_n)\}_{n=1}^{N}$, the estimate of g is given by $g(\hat{\boldsymbol{x}}_q) = \boldsymbol{\kappa}'^{\top}(\hat{\boldsymbol{x}}_q)\hat{\boldsymbol{\beta}}$ where $\boldsymbol{\kappa}'(\hat{\boldsymbol{x}}_q) :=$

$[\kappa'(\hat{\boldsymbol{x}}_q, \hat{\boldsymbol{x}}_1), ..., \kappa'(\hat{\boldsymbol{x}}_q, \hat{\boldsymbol{x}}_N)]^\top$, $\hat{\boldsymbol{\beta}} = (\mathbf{K}' + \lambda N \mathbf{I}_N)^{-1}\tilde{\boldsymbol{p}}$, and $\boldsymbol{K}'$ is an $N \times N$ matrix with (n, n')-th entry $\kappa'(\hat{\boldsymbol{x}}_n, \hat{\boldsymbol{x}}_{n'})$ and κ is a Gaussian radial basis function with $\sigma = 35$ m.

Quantitative evaluation will compare the normalized mean square error (NMSE) defined as

$$\text{NMSE} = \frac{\mathbb{E}\{|p(\boldsymbol{x}) - \hat{p}(\boldsymbol{Y}(\boldsymbol{x}) + \boldsymbol{\Upsilon}, \mathcal{T})|^2\}}{\mathbb{E}\{|p(\boldsymbol{x}) - \bar{p}|^2\}},$$

where $\boldsymbol{Y}(\boldsymbol{x})$ comprises the received pilot signals at location $\boldsymbol{x}$, $\boldsymbol{\Upsilon}$ represents noise, $\bar{p}$ is the spatial average of $p(\boldsymbol{x})$, and $\mathcal{T}$ is the training set, defined as $\mathcal{T} := \{(\boldsymbol{Y}_n + \boldsymbol{\Upsilon}_n, \tilde{p}_n + \epsilon_n)\}_{n=1}^N$ with $\boldsymbol{\Upsilon}_n$ and ϵ_n representing noise. Specifically, $\{\epsilon_n\}_{n=1}^N$ are independent log-normal random variables with zero-mean and standard deviation 0.5 dB ($\tilde{p}_n$ is measured in dBW). Furthermore $\mathbb{E}\{\cdot\}$ denotes expectation over a random location $\boldsymbol{x}$ uniformly distributed across $\mathcal{X}$, the locations of the sensors, and noise.

The true map generated through the canyon model is depicted to the left of Fig. A.1. The middle and right panels respectively show the localization-free and localization-based map estimates, which are obtained by placing a query sensor at each location. Black crosses indicate the positions of the N sensors used to estimate the map. As expected, the estimation is better in areas with more sensors. Visually, the quality of the localization-free estimate is higher than that of the localization-based estimate due to multipath.

Fig. A.2a shows the NMSE as a function of N for different numbers M of pilot signals. Each point is obtained by averaging 200 independent Monte Carlo iterations. As anticipated, performance improves with N. Furthermore, for fixed N, the NMSE is non-increasing with M, yet $M = 2$ and 3 yield roughly the same NMSE because of the geometry of the simulation setup.

Fig. A.2b shows the NMSE as a function of the number of sensors N used to estimate p^{LF} and p^{LB}. With significant evidence, one may claim that the proposed localization-free cartography scheme outperforms its localization-based counterpart when $N > 60$ since the error bars in Fig. A.2 span over 6 standard deviations of the NMSE across realizations. The reason for a poorer performance of the localization-based scheme is that multipath propagation can mislead the localization algorithm, inducing errors in location estimation that increase deviations in the map estimation as well.

A.5 Conclusions

Localization-free cartography has been proposed as an alternative to classic localization-based schemes, which do not operate properly when multipath impairs the propagation of localization pilot signals. Kernel-ridge regression was applied to estimate power maps from features of those pilot signals collected by a number of sensors. Simulations corroborate the merits of localization-free cartography relative to localization-based methods. Future research will include an extensive simulation study in indoor environments and develop distributed and online extensions.

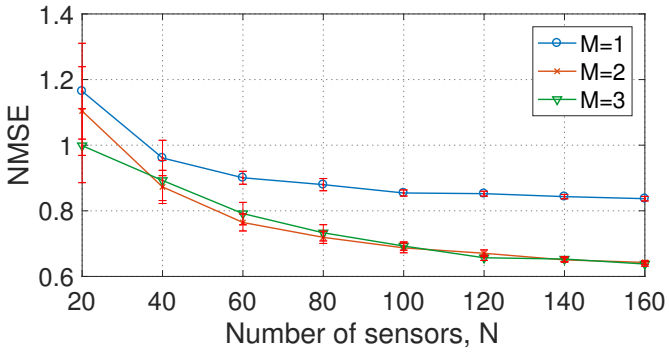

(a)

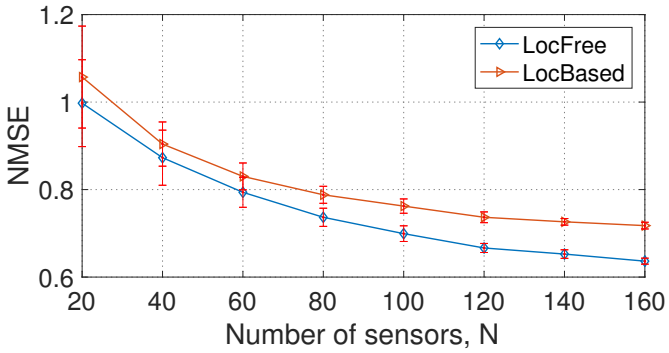

(b)

Figure A.2: (a) Estimated map NMSE for different values of number of features, M and sensors, N; and (b) Performance comparison between the localization-free cartography and the localization-based cartography ($\lambda = 3 \times 10^{-3}$,$\sigma = 30$ m).

References

[1] A. Alaya-Feki, S. B. Jemaa, B. Sayrac, P. Houze, and E. Moulines, "Informed spectrum usage in cognitive radio networks: Interference cartography," in *Proc. IEEE Int. Symp. Personal, Indoor Mobile Radio Commun.*, Cannes, France, Sep. 2008, pp. 1–5.

[2] J.-A. Bazerque and G. B. Giannakis, "Distributed spectrum sensing for cognitive radio networks by exploiting sparsity," *IEEE Trans. Signal Process.*, vol. 58, no. 3, pp. 1847–1862, Mar. 2010.

[3] B. A. Jayawickrama, E. Dutkiewicz, I. Oppermann, G. Fang, and J. Ding, "Improved performance of spectrum cartography based on compressive sensing in cognitive radio networks," in *Proc. IEEE Int. Commun. Conf.*, Budapest, Hungary, Jun. 2013, pp. 5657–5661.

[4] D. Romero, S-J. Kim, G. B. Giannakis, and R. López-Valcarce, "Learning power spectrum maps from quantized power measurements," *IEEE Trans. Signal Process.*, vol. 65, no. 10, pp. 2547–2560, May 2017.

[5] S. Grimoud, S. B. Jemaa, B. Sayrac, and E. Moulines, "A REM enabled soft frequency reuse scheme," in *Proc. IEEE Global Commun. Conf.*, Miami, FL, Dec. 2010, pp. 819–823.

[6] E. Dall'Anese, S.-J. Kim, G. B. Giannakis, and S. Pupolin, "Power control for cognitive radio networks under channel uncertainty," *IEEE Trans. Wireless Commun.*, vol. 10, no. 10, pp. 3541–3551, Aug. 2011.

[7] G. Boccolini, G. Hernandez-Penaloza, and B. Beferull-Lozano, "Wireless sensor network for spectrum cartography based on kriging interpolation," in *Proc. IEEE Int. Symp. Personal, Indoor Mobile Radio Commun.*, Sydney, NSW, Nov. 2012, pp. 1565–1570.

[8] W.C.M.V. Beers and J.P.C. Kleijnen, "Kriging interpolation in simulation: A survey," in *Proc. IEEE Winter Simulation Conf.*, Washington, D. C., Dec. 2004, vol. 1, pp. 113–121.

[9] G. Ding, J. Wang, Q. Wu, Y.-D. Yao, F. Song, and T. A Tsiftsis, "Cellular-base-station-assisted device-to-device communications in TV white space," *IEEE J. Sel. Areas Commun.*, vol. 34, no. 1, pp. 107–121, Jul. 2016.

[10] S.-J. Kim, N. Jain, G. B. Giannakis, and P. Forero, "Joint link learning and cognitive radio sensing," in *Proc. Asilomar Conf. Signal, Syst., Comput.*, Pacific Grove, CA, Nov. 2011, pp. 1415 –1419.

[11] S.-J. Kim and G. B. Giannakis, "Cognitive radio spectrum prediction using dictionary learning," in *Proc. IEEE Global Commun. Conf.*, Atlanta, GA, Dec. 2013, pp. 3206 – 3211.

[12] D.-H. Huang, S.-H. Wu, W.-R. Wu, and P.-H. Wang, "Cooperative radio source positioning and power map reconstruction: A sparse Bayesian learning approach," *IEEE Trans. Veh. Technol.*, vol. 64, no. 6, pp. 2318–2332, Aug. 2014.

[13] M. Hamid and B. Beferull-Lozano, "Non-parametric spectrum cartography using adaptive radial basis functions," in *Proc. IEEE Int. Conf. Acoust., Speech, Signal Process.*, New Orleans, LA, Mar. 2017, pp. 3599–3603.

[14] J.-A. Bazerque, G. Mateos, and G. B. Giannakis, "Group-lasso on splines for spectrum cartography," *IEEE Trans. Signal Process.*, vol. 59, no. 10, pp. 4648–4663, Oct. 2011.

[15] S.-J. Kim, E. Dall'Anese, and G. B. Giannakis, "Cooperative spectrum sensing for cognitive radios using kriged Kalman filtering," *IEEE J. Sel. Topics Signal Process.*, vol. 5, no. 1, pp. 24–36, feb. 2011.

[16] D. Romero, D. Lee, and G. B. Giannakis, "Blind channel gain cartography," in *Proc. IEEE Global Conf. Signal Inf. Process.*, Greater Washington, D. C., Dec. 2016, pp. 1110–1115.

[17] D. Lee, S.-J. Kim, and G. B. Giannakis, "Channel gain cartography for cognitive radios leveraging low rank and sparsity," *IEEE Trans. Wireless Commun.*, vol. 16, no. 9, pp. 5953–5966, Jun. 2017.

[18] M. Bshara, U. Orguner, F. Gustafsson, and L. Van Biesen, "Fingerprinting localization in wireless networks based on received-signal-strength measurements: A case study on WiMAX networks," *IEEE Trans. Veh. Technol.*, vol. 59, no. 1, pp. 283–294, Aug. 2009.

[19] B. Schölkopf, R. Herbrich, and A. J. Smola, "A generalized representer theorem," in *Proc. Comput. Learning Theory*, Amsterdam, The Netherlands, Jul. 2001, pp. 416–426.

[20] C. M. Bishop, *Pattern Recognition and Machine Learning*, Information Science and Statistics. Springer, 2006.

[21] F. Pérez Fontán and P. Mariño Espiñeira, *Modeling the wireless propagation channel: a simulation approach with Matlab*, Wiley, 2008.

[22] J.-A. Bazerque and G. B. Giannakis, "Nonparametric basis pursuit via kernel-based learning," *IEEE Signal Process. Mag.*, vol. 28, no. 30, pp. 112–125, Jul. 2013.

[23] C. A. Micchelli, Y. Xu, and H. Zhang, "Universal kernels," *J. Mach. Learn. Res.*, vol. 7, pp. 2651–2667, Dec. 2006.

[24] A. Beck, P. Stoica, and J. Li, ," *IEEE Trans. Signal Process.*, vol. 56, no. 5, pp. 1770–1778, 2008.